Egypt. J. Chem. **Vol. 65,** No. 10 pp. 209 - 215 (2022)

Egyptian Journal of Chemistry

http://ejchem.journals.ekb.eg/

Surface Decoration of Zirconium Oxide with Bismuth sulfide Catalysts for Photocatalytic Degradation of Red dye 195

Heba K. El- El-Kholly [*1], Shimaa M. Abdel Moneim[1], Hanan S. Ibrahim[1], Nabila S. Ammar[1], Ahmed G. El-Deen[2], M H. Helal[3], M K. Zahran[3], Mohammed Eid M. Ali1

1 Water Pollution Research Department, National Research Center, El-Buhouth St., Dokki, Cairo, Egypt P.O. 12622

2 Renewable Energy Science and Engineering Department, Faculty of Postgraduate Studies for Advanced Sciences (PSAS), Beni-Suef University, Beni-Suef 62511, Egypt

3 Chemistry Department, Faculty of Science, Helwan University, Ain-Helwan, Cairo, Egypt

Abstract

Recently, solar energy has been considered the most vulnerable source to resolve environmental pollution and energy scarcity problems. Researchers have made intense research efforts to convert solar energy into chemical energy through photocatalysis processes as it is a green, clean, and renewable energy source. Numerous discovered photocatalysts show absorption in the ultraviolet–visible (UV~5% and visible ~43%) region. Zirconia based material is a noteworthy metal oxide because of its characteristics. It can be implemented in different applications; photocatalytic oxidation for dye degradation. The main focus of this research was to synthesize Bi_2S_3@ZrO_2 from low cost and locally available materials, zircon, in addition to preparation of ZrO_2 bismuth catalyst of different concentration. Characterization of prepared materials was performed using X-ray diffraction (XRD), Fourier transform infrared spectra (FTIR), and scanning electron microscope (SEM). The results confirmed that the homogeneous spherical particles were produced. Moreover, different ratios, 5% Bi_2S_3@ZrO_2, 7% Bi_2S_3@ZrO_2, and 10% Bi_2S_3@ZrO_2, were investigated against removal of Red dye using adsorption and photocatalytic activities. As obtained, the removal adsorptive capacity for red dye 195 was decreased in the range from 144 to 88 mg/g using 0.2 g/L of prepared hybrids. However, 5% Bi_2S_3@ZrO_2 showed the highest photodegradation of Red dye. Meanwhile, red dye was removed with rate constant of 0.132 - 0.324 h^{-1} under solar simulator. Kinetic studies indicate that the removal efficiency depends on the dye concentration. This work opens the way for high efficient adsorbents and photocatalysts for wastewater treatment.

Keywords: Zircounim oxide; Bismuth sulfide; Red dye; Photocatalysis; Degradation

Introduction

Recently, water decontamination becomes an urgent need to overcome the shortage in fresh water due to the increment of population and wealth concerns [1]. Dyes are one of the most serious contaminants that have a negative impact on the environment [2]. These coloring agents can be continuously released from different sources such as textile and tanning drains [3]. Particularly, azo-dyes "eg. Red dye 195" are hazardous organic pollutants, chemically stable, non-biodegradable, and difficultly to be degraded from wastewater [4-6]. Therefore, current research focuses to develop high efficient materials have strong degradation or removal power in order to get rides these effluents. Also, several strategies have been reported such as chemical, physical, and biological treatments [7-10]. However, advanced oxidation approaches, like photocatalysis, greatly paid the attention of researchers compared to other techniques that usually generate secondary impurities due to the high efficiency to purify wastewater from the organic contaminants [11, 12]. Moreover, this technique has a wide range of applications in terms of superior performance, safe, inexpensive, and can be considered as a promising technology in elimination of exhaust emissions using an eco-friendly pathway [13-15].

Typically, the photodegradation of dye relies on absorption of high energy photons of specific wave length by a photocatalyst [14]. This leads to excitation of the electrons from the valance band to the

*Corresponding author e-mail hebakelkholly@gmail.com

Receive Date: 30 December 2021, Revise Date: 10 January 2022, Accept Date: 11 January 2022

DOI: 10.21608/EJCHEM.2022.113846.5171

conduction band forming holes and photoinduced electrons, respectively. These electrons can migrate to the material' surface causing reduction of the adsorbed oxygen to form O-2. Meanwhile, the adsorbed water molecules can be oxidized via created holes in the valence band to form hydroxyl radical (OH•) which have a strong oxidation potential (2.8 eV). These reactive oxygen species are responsible for degradation of the adsorbed dye molecules [16]. Zirconia or ZrO2 is one of the robust catalysts that has superior physicochemical properties unlike other transition metal/metal oxides such as high thermal stability, high mechanical strength, large surface area and particle size, unique polymorphic crystalline structure, short ionic radius, well-distributed charges, spherical electron orbital, acidic-basic duel functions, oxidizing-reducing ability, tetravalent characters, and ability to form various stable coordinate compounds [17, 18]. Therefore, zirconium oxide has been enrolled in several environmental applications as adsorbents, coagulants, photocatalyst, etc. Nevertheless, zirconia suffers from a wide energy gap (~ 5.25 eV) which limits its applications as a photocatalyst [19]. Thus, researchers got the challenge to reduce this value utilizing various strategies, such as creating structural surface defects or doping with other materials [20]. In the last technique, addition of metal/metal oxides as dopants, ex. Fe, Cu, Ag, TiO2, SnO2, and ZnO, could support the electron transfer process during the photocatalytic reaction which in turn improves the photocatalytic activity of the whole system [21-23].

On the other hand, bismuth-based materials showed strong applicability in the field of water treatment since these compounds enjoy relatively narrow band gap that facilitate absorption of not only visible-light but also UV photons [24]. Particularly, bismuth sulfide (mineral bismuthinite, Bi2S3) is among common bismuth chalcogenides [25]. It is a non-toxic substance has a lamellar 1D structure linked together by weak Bi-S bonds [26]. However, this compound is anisiotropic in nature since Bi3+and S2- ions are arranged above each other in an orthorhombic cell structure of [001] reflection plane along infinite chains [27]. Furthermore, these compounds have unique properties; density of 6.807 g/cm3, intrinsic carrier concentration of 3 ×1018cm-3, carrier mobility of 200 cm2/Vs, electrical conductivity in the range from 10-6 to10-7 Ω cm-1, hole mobility of 1100 cm2/Vs, and the refractive index of 589.3 nm [27]. Strikingly, Bi2S3 is a promising active n-type V-VI semiconductor of a narrow band gap (~1.3 eV) compared to other metal oxide semiconductors [25]. Therefore, it finds a strong workability in the photocatalysis [28].

No doubt, decoration of zirconia with bismuth sulfide would play a crucial role in the reduction of the electron–hole recombination but also balance the charge on the catalyst surface. This could improve adsorption of more hydroxide ions and block the recombination of electron–hole pairs. This article presents an approach for the synthesis of new catalyst based zirconia. In the present work, a low cost photocatalyst was prepared via the doping of zircounim with bismuth sulfite in order to obtain a catalyst with improved properties. To award further advantages for the prepared hybrids with different concentrations of Bi2S3@ZrO2 catalyst, the ease preparation via in-situ ultrasonic technique could be achieved. Finally, the prepared samples were characterized and evaluated under photoreactor conditions against removal of Red dye 195.

1. Experimental

2.1. Materials

Red dye (98%), thiourea (97.5 %), sodium hydroxide (98%), and bismuth nitrate (98%) were provided from sigma Aldrich (USA) used without further treatment and zirconium oxide (zro_2-500) prepared from zircon [29].

2.2. Preparation of Modified (Bi_2S_3@ZrO_2)

The novel hybrid of Bi_2S_3@ZrO_2 catalyst was successfully prepared from zircon as a low cost material. Certain weights of zirconium oxide and thiourea were mixed and suspend in 50 ml distilled water in presence of different amount of $Bi(NO_3)_2$. After ultra-sonication, 5 ml of 10 N NaOH were added for 10 min. Then, the resulted mixture was calcinated at 500ºC for 2 h in order to obtain different ratio of hybrid Bi_2S_3@ZrO_2 are illustrate in Table 1.

Table 1: Ratios of Bi_2S_3: ZrO_2 in the prepared hybrids

Composition	Ratio of ZrO_2 to dopant
5% Bi_2S_3@ZrO_2	95 % ZrO_2 / 5% Bi_2S_3
7% Bi_2S_3@ZrO_2	93 % ZrO_2 / 7% Bi2S_3
10% Bi_2S_3@ZrO_2	90 % ZrO_2 / 10% Bi_2S_3

2.3. Techniques

As generally known, the photocatalysts are favorable to be in a crystalline form which is the active phase required for the degradation of organic

contaminants. Therefore, crystallization behaviors of the prepared catalysts were examined by XRD technique; Bruker diffractometer (Germany) with graphite monochromatized (Cu-Kα) radiation (λ = 1.5406 Å). The patterns were collected in the 2θ range 10 – 70 with step of 0.05°. Moreover, the crystalline phases were identified by comparing the collected patterns with the standard ASTM cards. The crystallite size (L) of the prepared hybrids was also calculated using Scherer formula [30] as follows: β = (k ʎ)/(L cosθ) where, K is a constant (0.9), λ is wave length of X-ray source (0.1540598 nm), β is full width at half maximum in radians, and θ is Bragg´s diffraction angle.

Scanning electron microscope images were taken with SEM Model Quanta 250 FEG (Field Emission Gun) as mentioned elsewhere [31]. The chemical structure of the obtained hybrids was confirmed with FTIR spectrophotometer 630-JASCO (UK). In this analysis, 2 mg of the prepared powder were mixed with 100 mg of KBr and compressed into small disks. The spectra were recorded in the wave number range from 400 to 4000 cm^{-1}.

2.4. Adsorption batch

All adsorption trials were conducted on suitable diluted solution of Red dye 195 for 30 min under dark conditions. Mixture pH was adjusted to the proper value with 0.1 M HCl and 0.1 M NaOH solutions. The mixtures were shaken by shaker (Stuart scientific, UK) at 250 rpm. For photodegradation of dye, the photocatalyst was added to the dye solution and stirred in dark prior to the experiment in order to allow adsorption equilibrium. Then, the photoreactor (UVCUBE 400) was switched on to start the degradation process. The withdrawn samples in all experiments were passed through a syringe filter (PTFE, 0.45 µm) to separate the dispersed catalyst. Then, the intensity of residual dye in the filtrate was determined with a JASCO spectrophotometer (Model V730, Japan). The spectra were taken in the range from 200 to 700 nm. All the experiments were conducted in triplicates and the mean of results were used for further calculations. Moreover, the control experiment, i.e. photodegradation of dye in absence of photocatalyst, was performed to investigate photolysis of dye in water.

The uptake of pollutant by sorbent (q) is defined as the amount of pollutant in (mg) bound to one g of sorbent according to the following equation (1):

$$q\left(\frac{mg}{g}\right) = \frac{(C_i - C_e) \times V}{m} \qquad \text{Eq. (1)}$$

Where, "m" is the catalyst mass (g), "V" is the pollutant solution volume (L) in contact with the catalyst, "C_i" and "C_e" are the initial and equilibrium pollutant concentration (mg/L), respectively. Also, the percentage removal of pollutant was calculated according to Eq. (2):

$$\% R = \frac{(C_i - C_e)}{C_i} \times 100 \qquad \text{Eq. (2)}$$

3. Results and discussion

3.1. Fourier Transform Infrared (FTIR)

Fourier transform infrared spectroscopy was used in order to verify the functional groups on the catalyst backbone. Figure 1 showed FTIR spectra of the prepared zirconium dioxide and its hybrids. The characteristic IR bands of all samples were observed at 3020-3680 cm^{-1} and 1620 cm^{-1} corresponding to the stretching and bending vibrations of the O–H bond, respectively, due to the adsorbed water molecules. The peak at 1384 cm^{-1} with a low intensity is attributed to the non-bridging OH groups. However, the sharp and intense symmetric vibrational band of Zr–O bands was pronounced at 1033 cm^{-1}, meanwhile, the asymmetric one was detected broad in the region from 420 to 495 cm^{-1}[32]. Another broad peak at 684 cm^{-1} is ascribed to tetragonal phase of ZrO_2. On the other hand, the FTIR spectra of prepared Bi_2S_3/ZrO_2 hybrids of different ratios show peaks between 500-900 cm^{-1} were observed that assigned to coexistence of Bi_2S_3 in the same figure. The results indicate the existence of ZrO_2 in the prepared hybrids as the characteristic bands were observed between 400 and 900 cm^{-1}. As well absorption IR bands had shifts comparing to IR of ZrO_2 reference, confirming the doping effect of Bi_2S_3.

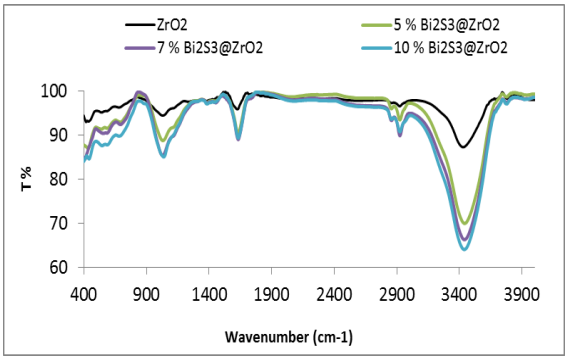

Figure1: FTIR spectra of prepared Bi_2S_3 doped ZrO_2 materials and reference ZrO_2

3.2. X-ray Diffraction (XRD)

To confirm the phase formation, XRD pattern for the prepared catalyst was recorded after calcinations at 500 ºC (Figure 2). The diffraction peaks designated presence of tetragonal phase

structure ZrO_2 materials according to (t-ZrO_2, JCPDS no. 89–7710). Other diffraction lines were observed at 2θ of 14.4° and 16.39° according to the standard diffraction data of Bi_2S_3 (JCPDS no. 17-0320). The narrow line widths indicate high crystalline nature of the synthesized material. It was found that, the strongest lines, at 2θ of 27.38º, 35.9 º, and 56.3º, are referred to [111] reflection plane of monoclinic phase. However, the spectra line at 2θ of 35.9º is revealed to [111] reflection plane of tetragonal phases. The crystallite size of prepared materials were found with range from 28.5 to 47.5 nm, meanwhile, the crystallite size of commercial Bi_2S_3@ZrO_2 was found 90 nm. The obtained XRD results confirmed the successful achievement of crystalline Bi_2S_3@ZrO_2 hybrids from ZrO_2 as low cost materials.

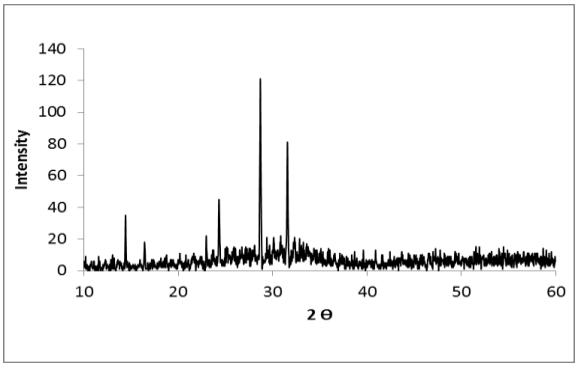

Figure 2: XRD pattern of Bi_2S_3@ZrO_2 hybrid catalyst

3.3. Scanning Electron Microscope (SEM)

In order to confirm the morphology of prepared Bi_2S_3-ZrO_2 hybrids, scanning electron microscopy imaging was carried out. Figure 3 depicted the typical SEM images for as-prepared catalysts at different ratio. The micrographs display the homogeneous assemblies of Bi_2S_3-ZrO_2 spherical particles. Increasing Bi_2S_3 concentration has led to altering the morphology of ZrO_2, by decreasing the agglomeration of granular shape due to the deposition of Bi_2S_3 on zirconium surface, which confirms successful preparation procedures.

3.4. Adsorption Efficiency

As well the adsorption profile of dye over prepared hybrid catalysts of different doping ratios (5, 7, and 10%) was depicted in Figure 4. As shown, Bi_2S_3@ZrO_2 materials demonstrate high adsorption capacity towards red dye. However, 10 % Bi_2S_3/ZrO_2 composition showed the highest removal which might be attributed to the presence of positively charged Bi_2S_3 of higher concentrations than others. This facilitates the chemical interaction with the negatively charged dye molecules [30].

Figure 3: SEM of Bi_2S_3 doped ZrO_2 catalyst [A] 5 % Bi_2S_3@ZrO_2, [B] 7 % Bi_2S_3@ZrO_2, and [C] 10 % Bi_2S_3@ZrO_2

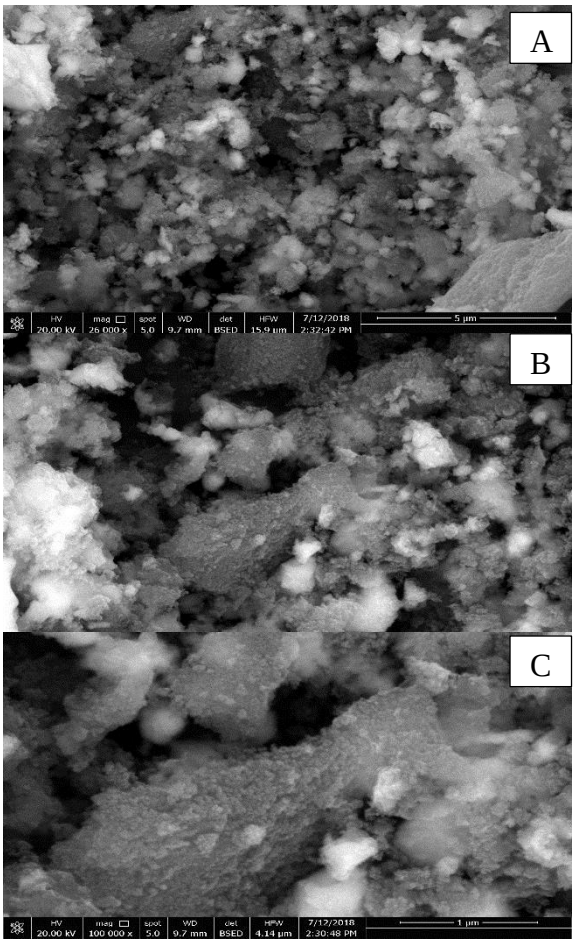

Figure 4: Adsorption removal capacity of red dye from wastewater using [A] 5 % Bi_2S_3@ZrO_2, [B] 7 % Bi_2S_3@ZrO_2, and [C] 10 % Bi_2S_3@ZrO_2 (Initial Conc. of dye = 50 mg/L)

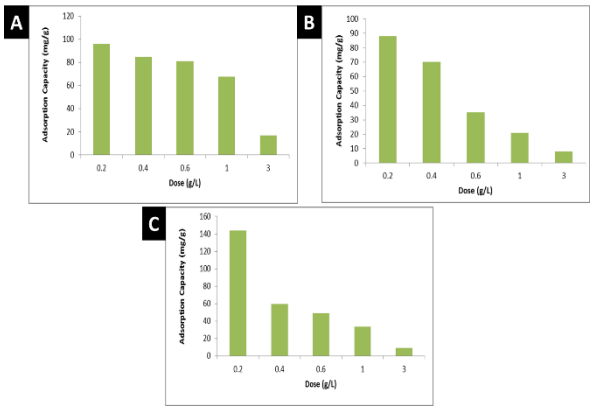

3.5 Photocatalysis under Sunlight Simulator

The experimental results showed that, there is no remarkable removal of dye from wastewater via photolysis under light irradiation. Thus, the presence

of light and **prepared** $Bi_2S_3@ZrO_2$ photocatalyst enhanced the photo-oxidation of dye. Figure 5 exhibited the photocatalytic removal of Red dye from wastewater using different dose of $Bi_2S_3@ZrO_2$ of different x % $Bi_2S_3@ZrO_2$ (x=5, 7, 10) under simulated sunlight at initial dye concentration of 50 mg/L. As seen from figure 5, the degradation rate of dye under simulated sunlight was increased with reaction time and with increasing the photocatalyst dose. Also, the maximum removal percentage of dye was amounted by 66 %, 64 %, and 62 % for 5 % $Bi_2S_3@ZrO_2$, 7 % $Bi_2S_3@ZrO_2$, and 10 % $Bi_2S_3@ZrO_2$, respectively, after 120 min of irradiation using 1 g/L of photocatalyst. As a result, the efficiency of ZrO_2 was enhanced by introducing Bi_2S_3.

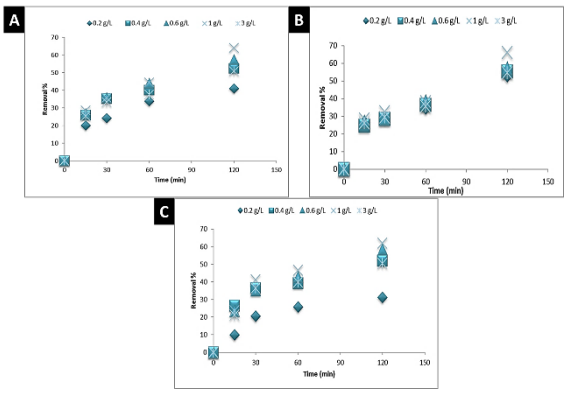

Figure 5: Photocatalytic removal of dye from wastewater using [A] 7 % $Bi_2S_3@ZrO_2$, [B] 5 % $Bi_2S_3@ZrO_2$, and [C] 10 % $Bi_2S_3@ZrO_2$ (initial Conc of dye = 50 mg/L)

3.6 Kinetic Studies for Photocatalytic Degradation Process

To fully understand any chemical reaction, not only the identities of the reactants and the products must be known, but also, how long the reaction will take to occur (i.e., is it kinetically feasible). The reaction time is also very important parameter in the design of treatment plant. In other words, it is important to know the retention time of the reaction in the tank. Therefore, the objective was directed to the kinetics evaluation of the photo-degradation process of the dye over prepared $Bi_2S_3@ZrO_2$ catalysts. Chemical kinetics addresses important issues in heterogeneous photocatalysis.

The rate of reaction is measured based on the property that is easiest to measure. This property can be concentration. As several products of varied structure and quantity can be formed during photocatalytic reactions, it is more convenient to measure reaction rates based on the disappearance of such a property. The rate of disappearance of dye can be given by differential rate equation known as the differential rate law. A general differential rate law was previously reported [33]. From engineering point of view, it is useful to find out exact rate equation that fits the experimental rate data. So, the kinetics of heterogeneous photocatalytic reaction was studied extensively.

The zero, half, first, and second order reaction kinetics were applied for the photocatalytic degradation of dye over the prepared materials under sunlight irradiation. The calculated kinetic parameters are tabulated in Table 2, Table 3 and Table 4 respectively.

Although the experimental results of photocatalytic degradation of dye have a good fitting with zero and half reaction model for ZrO_2 at different catalyst dose, it showed moderate fitting for 5 % $Bi_2S_3@ZrO_2$, 7 % $Bi_2S_3@ZrO_2$, and 10 % $Bi_2S_3@ZrO_2$. The corresponding calculated $t_{1/2}$ for zero and half reaction model is not matched with the experimental findings. Thus, the photocatalytic degradation of dye does not follow the zero and half order reaction. Pseudo-first and pseudo-second order reaction showed a good fitting with experimental results. The corresponding calculated half-life times of dye decomposition ranged from 82 min to 141 min for pseudo first-order which is in a good agreement with the experimental time of dye degradation. Meanwhile, based on pseudo second rate constant, the calculated half-life times of dye decomposition ranged from 66 min to 282 min is in moderately agreement with the experimental time of dye degradation. In general, the removal of dye from aqueous solution by the prepared materials is better described by the first-order kinetics, i.e. the removal depends on the concentration of dye.

Table 2: Calculated kinetic parameters for photocatalytic degradation of dye under simulated sunlight using 5 % $Bi_2S_3@ZrO_2$

Material	dose g/L	Zero			Half			First			Second		
		k^0/ 1000	R^2	$t^{1/2}$	$k^{1/2}$/ 1000	R^2	$t^{1/2}$	k1/ 1000	R^2	$t^{1/2}$	k^2/ 1000	R^2	$t^{1/2}$
5 % $Bi_2S_3@ZrO_2$	0.2	195.1	0.81	256	16.8	0.923	248	9.8	0.87	120	0.18	0.99	111
	0.4	201.7	0.84	248	17.5	0.9	238	11.1	0.87	98	0.196	0.97	102
	0.6	193.4	0.76	259	17	0.88	245	16.3	0.97	89	0.198	0.992	101
	1	227.7	0.78	220	21	0.81	199	17.9	0.942	82	0.302	0.97	66
	3	196	0.89	255	16.8	0.86	248	11.7	0.85	90	0.188	0.96	106

Table 3: The calculated kinetic parameters of photocatalytic degradation of dye under simulated sunlight using 7 % $Bi_2S_3@ZrO_2$

Material	dose g/L	Zero			Half			First			Second		
		$k^0/1000$	R^2	$t^{1/2}$	$k^{1/2}/1000$	R^2	$t^{1/2}$	$k^1/1000$	R^2	$t^{1/2}$	$k^2/1000$	R^2	$t^{1/2}$
7% $Bi_2S_3@ZrO_2$	0.2	145.7	0.78	343	11.8	0.81	354	9.2	0.88	133	0.105	0.9	190
	0.4	185	0.79	270	15.8	0.84	264	13.4	0.97	107	0.168	0.95	119
	0.6	203.4	0.81	246	17.8	0.86	234	14.8	0.972	94	0.209	0.98	96
	1	229.8	0.89	218	20.9	0.91	200	15	0.96	91	0.28	0.98	71
	3	176.2	0.83	284	15.5	0.87	269	10.6	0.833	100	0.155	0.95	129

Table 4: The calculated kinetic parameters of photocatalytic degradation of dye under simulated sunlight using 10 % $Bi_2S_3@ZrO_2$

Material	Dose g/L	Zero			Half			First			Second		
		$k^0/1000$	R^2	$t^{1/2}$	$k^{1/2}/1000$	R^2	$t^{1/2}$	$K^1/000$	R^2	$t^{1/2}$	$k^2/1000$	R^2	$t^{1/2}$
10 % $Bi_2S_3@ZrO_2$	0.2	117.4	0.79	426	9.2	0.81	453	4.9	0.91	141	0.071	0.6	282
	0.4	174.7	0.73	286	14.9	0.77	280	7.7	0.86	122	0.158	0.9	127
	0.6	210.4	0.83	238	18.5	0.88	226	8.9	0.9	110	0.22	0.977	91
	1	225.4	0.79	222	20.2	0.84	207	11.1	0.93	98	0.259	0.964	77
	3	180.9	0.73	276	15.3	0.77	273	9.1	0.891	114	0.159	0.88	126

4. Conclusions

Different ratios of $Bi_2S_3@ZrO_2$ were successfully prepared from low cost and locally available materials using ultra-sonication technique. XRD showed highly crystalline feature of prepared catalyst and increasing of crystallite size. FTIR confirmed successful interaction within the hybrid catalysts. SEM images displayed homogenous spherical particles of $Bi_2S_3@ZrO_2$. Moreover, 5% $Bi_2S_3@ZrO_2$ showed the highest removal of Red dye using adsorption and photocatalytic activities. The removal adsorptive capacity for red dye 195 was decreased from 144 to 88 mg/g with 0.2 g/L of 5% Bi_2S_3-ZrO_2, 7% $Bi_2S_3@ZrO_2$, and 10% $Bi_2S_3@ZrO_2$. Meanwhile, red dye was removed with rate constant of 0.132 - 0.324 h^{-1} under solar simulator. Kinetics models emphasized that the removal of dye from aqueous solution by the prepared materials is better described by the first-order.

Acknowledgment

The authors are grateful to national research centre for financial support of project entitled "**Development of effective low-cost materials for removing hazardous contaminants from industrial wastewater** " Fund grant No.#. 11070105

References

1. Sikosana, M.L., et al., Municipal wastewater treatment technologies: A review. Procedia Manufacturing, 2019. 35: p. 1018-1024.
2. Dutta, S., et al., Recent advances on the removal of dyes from wastewater using various adsorbents: a critical review. Materials Advances, 2021.
3. Benkhaya, S., S. M'rabet, and A. El Harfi., A review on classifications, recent synthesis and applications of textile dyes. Inorganic Chemistry Communications, 2020. 115: p. 107891.
4. Chung, K.-T., Azo dyes and human health: a review. Journal of Environmental Science and Health, Part C, 2016. 34(4): p. 233-261.
5. Selvaraj, V., et al., An over review on recently developed techniques, mechanisms and intermediate involved in the advanced azo dye degradation for industrial applications. Journal of molecular structure, 2021. 1224: p. 129195.
6. Suzuki, M., et al., Biological treatment of non-biodegradable azo-dye enhanced by zero-valent iron (ZVI) pre-treatment. Chemosphere, 2020. 259: p. 127470.
7. Aksakal, O. and H. Ucun, Equilibrium, kinetic and thermodynamic studies of the biosorption of textile dye (Reactive Red 195) onto Pinus sylvestris L. Journal of hazardous materials, 2010. 181(1-3): p. 666-672.
8. Donkadokula, N.Y., et al., A review on advanced physico-chemical and biological textile dye wastewater treatment techniques. Reviews in environmental science and bio/technology, 2020: p. 1-18.
9. Piaskowski, K., R. Świderska-Dąbrowska, and P.K. Zarzycki., Dye removal from water and

wastewater using various physical, chemical, and biological processes. Journal of AOAC International, 2018. 101(5): p. 1371-1384.
10. Doma, H. S., El-Kamah, H. M., and El-Qelish, M., Slaughterhouse wastewater treatment using UASB reactor followed by down flow hanging sponge unit. Research journal of pharmaceutical biological and chemical sciences, 2016. 7(2), 568-576.
11. Chan, S.H.S., et al., Recent developments of metal oxide semiconductors as photocatalysts in advanced oxidation processes (AOPs) for treatment of dye waste-water. Journal of Chemical Technology & Biotechnology, 2011. 86(9): p. 1130-1158.
12. Nidheesh, P., M. Zhou, and M.A. Oturan., An overview on the removal of synthetic dyes from water by electrochemical advanced oxidation processes. Chemosphere, 2018. 197: p. 210-227.
13. Konstantinou, I.K. and T.A. Albanis., TiO_2-assisted photocatalytic degradation of azo dyes in aqueous solution: kinetic and mechanistic investigations: a review. Applied Catalysis B: Environmental, 2004. 49(1): p. 1-14.
14. Rauf, M. and S.S. Ashraf., Fundamental principles and application of heterogeneous photocatalytic degradation of dyes in solution. Chemical engineering journal, 2009. 151(1-3): p. 10-18.
15. Anwer, H., et al., Photocatalysts for degradation of dyes in industrial effluents: Opportunities and challenges. Nano Research, 2019. 12(5): p. 955-972.
16. Nazri, M.K.H.M. and N. Sapawe., A short review on photocatalytic toward dye degradation. Materials Today: Proceedings, 2020. 31: p. A42-A47.
17. Asharaf, S., Karthigeyan, A. S., Deivanai, M., & Mani, R., Zirconia: properties and application" a review. Pakistan Oral & Dental Journal, 2014, 34(1).
18. Saridag, S., O. Tak, and G. Alniacik., Basic properties and types of zirconia: An overview. World Journal of Stomatology, 2013. 2(3): p. 40-47.
19. Ali, M.E.M., et al., Production of zirconia materials from zircon for dye removal from wastewater. Egyptian Journal of Chemistry, 2020. 63(2): p. 515-523.
20. Długosz, O., K. Szostak, and M. Banach., Photocatalytic properties of zirconium oxide–zinc oxide nanoparticles synthesised using microwave irradiation. Applied Nanoscience, 2020. 10(3): p. 941-954.
21. Aghabeygi, S. and M. Khademi-Shamami., ZnO/ZrO_2 nanocomposite: Sonosynthesis, characterization and its application for wastewater treatment. Ultrasonics sonochemistry, 2018. 41: p. 458-465.
22. Pirzada, B.M., et al., Synthesis, characterization and optimization of photocatalytic activity of TiO_2/ZrO_2 nanocomposite heterostructures. Materials Science and Engineering: B, 2015. 193: p. 137-145.
23. López, U., Lemus, A., Hidalgo, M. C., López González, R., Quintana Owen, P., Oros-Ruiz, S., and Acosta, J., Synthesis and characterization of ZnO-ZrO2 nanocomposites for photocatalytic degradation and mineralization of phenol. Journal of Nanomaterials, 2019.
24. Wei, X., et al., A review on bismuth oxyhalide based materials for photocatalysis. Nanoscale Advances, 2021. 3(12): p. 3353-3372.
25. Sharma, S., and Khare, N., Synthesis of bismuth sulfide nanostructures for photodegradation of organic dye. In AIP Conference Proceedings (Vol. 1832, No. 1, p. 050064). AIP Publishing LLC.
26. Biswas, K., L.D. Zhao, and M.G. Kanatzidis., Tellurium-Free Thermoelectric: The Anisotropic n-Type Semiconductor Bi_2S_3. Advanced Energy Materials, 2012. 2(6): p. 634-638.
27. Ajiboye, T.O. & D.C. Onwudiwe., Bismuth sulfide based compounds: properties, synthesis and applications. Results in Chemistry, 2021: p. 100151.
28. Sahu, H. R., & Rao, G. R., Characterization of combustion synthesized zirconia powder by UV-vis, IR and other techniques. *Bulletin of Materials Science*, 2000, *23*(5), 349-354.
29. Mohammed Eid M. Ali, Shimaa, M, Abdel Moneim, Hanan S. Ibrahim, Nabila S. Ammar, Heba K. El-Kholly, Ahmed G. El-Deen, M K. Zahran, & M H. Helal., Production of zirconia materials from zircon for dye removal from wastewater. Egyptian Journal of Chemistry, 2020, 63, 515-523.
30. Abdel-Moniem, S. M., El-Liethy, M. A., Ibrahim, H. S., & Ali, M. E., Innovative green/non-toxic Bi_2S_3@ g-C_3N_4 nanosheets for dark antimicrobial activity and photocatalytic depollution: Turnover assessment. Ecotoxicology and Environmental Safety, 2021, 226, 112808.
31. El-Qelish, M., and Mahmoud, M., Overcoming organic matter limitation enables high nutrient recovery from sewage sludge reject water in a self-powered microbial nutrient recovery cell. Science of the Total Environment, 2022, 802, 149851.
32. B.D. Cullity., Publishing Cos, 2nd ed., Addison-Wesley, Reading, MA, 1978, pp. 102
33. José J.C. Teixeira-Dias., Biochemical Impact of Platinum and Palladium-based Anticancer Agents, Chemical Kinetics, In book: Molecular Physical Chemistry, 2017 (pp.83-111)